Supplementary Figure 1

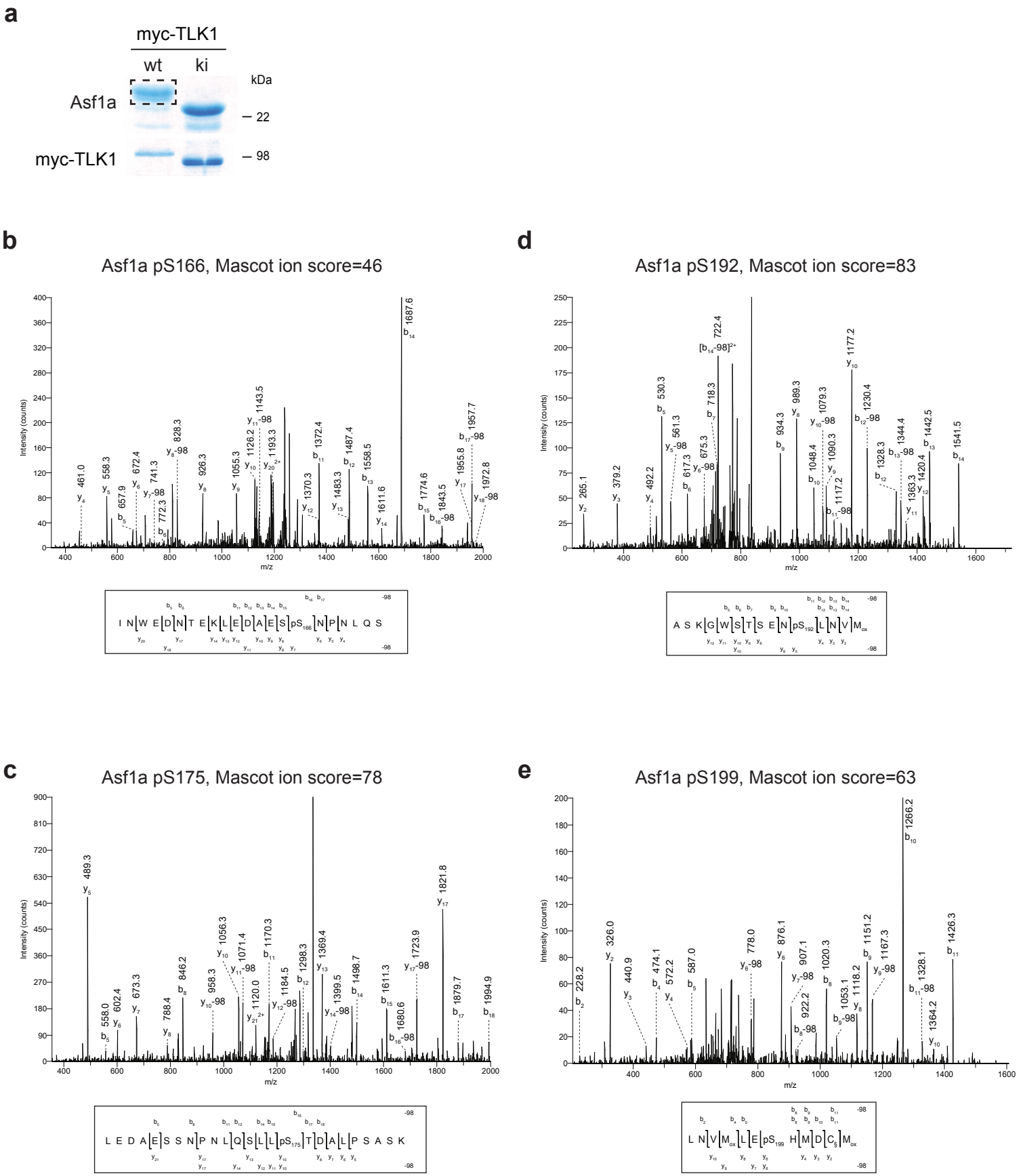

Supplementary Figure 1. Mass spectrometry analysis of Asf1a sites phosphorylated by TLK1 *in vitro*. **(a)** Coomassie staining of recombinant Asf1a phosphorylated *in vitro* by recombinant myc-TLK1 wild-type (wt) or kinase-inactive (ki) mutant. The Asf1a band (highlighted by dashed box) with potentially phosphorylated forms was subjected to mass spectrometry analysis (LC-MS/MS). **(b-e)** MS/MS spectra of the samples described in (a) depicts phosphorylation at the Asf1a peptide containing pS166 (b), pS175 (c), pS192 (d), pS199 (e). Observed b- and y-ions, as well as those resulting from the neutral loss of H_3PO_4 (-98 Da), are indicated in the spectrum and peptide sequence. $C_{\S}$ denotes a carbamidomethylated cysteine, while an oxidized methionine is represented by M_{ox}.

Supplementary Figure 2

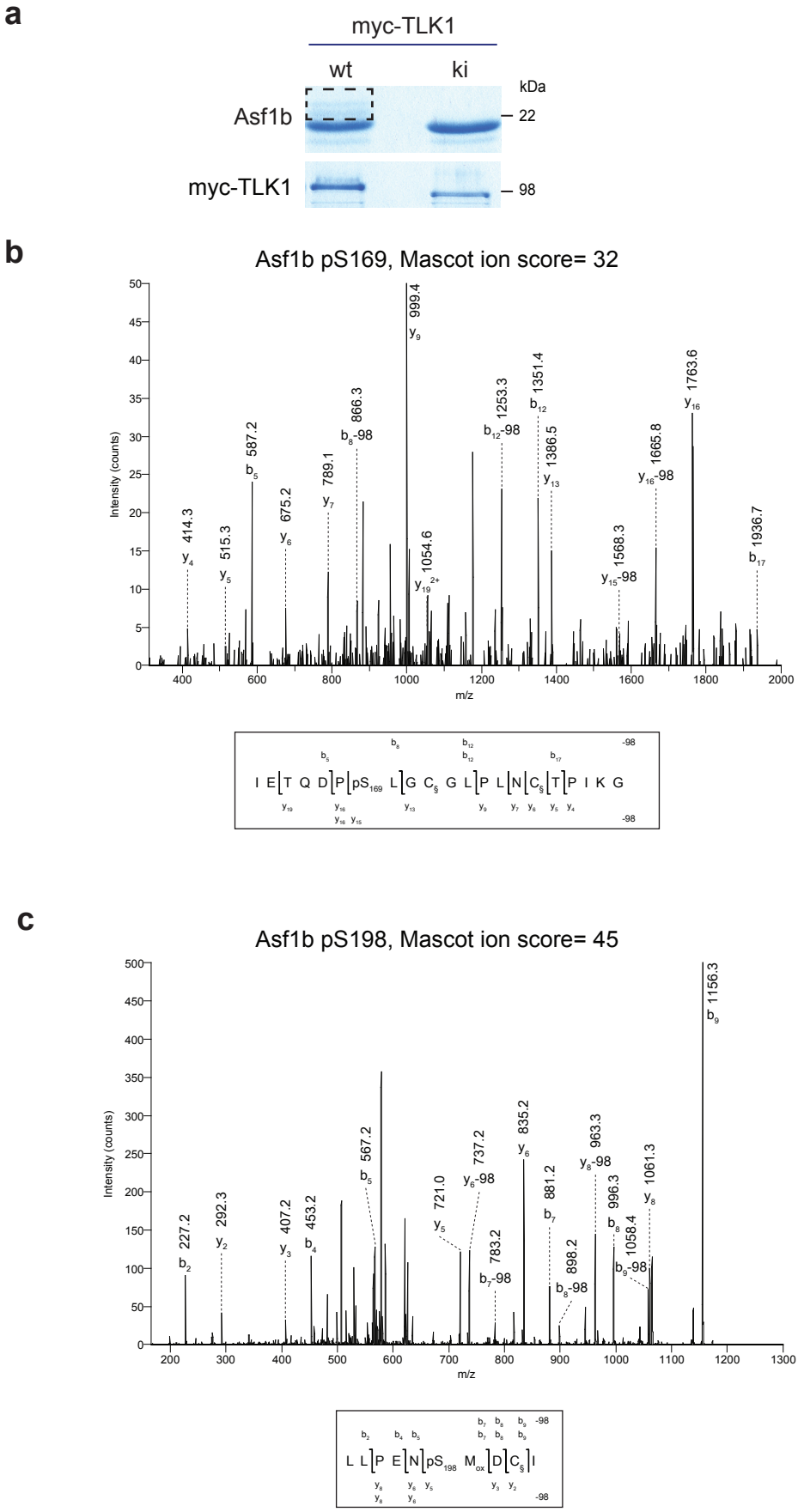

Supplementary Figure 2. Mass spectrometry analysis of Asf1b sites phosphorylated by TLK1 *in vitro*. **(a)** Coomassie staining of recombinant Asf1b phosphorylated in vitro by recombinant myc-TLK1 wild-type (wt) or kinase-inactive (ki) mutant. The Asf1b band (boxed) with potentially phosphorylated forms was subjected to mass spectrometry analysis (LC-MS/MS). **(b, c)** MS/MS spectra of the samples described in (a) depicts phosphorylation at the Asf1b peptide containing pS169 (b) and pS198 (c). Observed b- and y-ions, as well as those resulting from the neutral loss of H_3PO_4 (-98 Da), are indicated in the spectrum and peptide sequence. $C_§$ denotes a carbamidomethylated cysteine, while an oxidized methionine is represented by M_{ox}.

Supplementary Figure 3

a

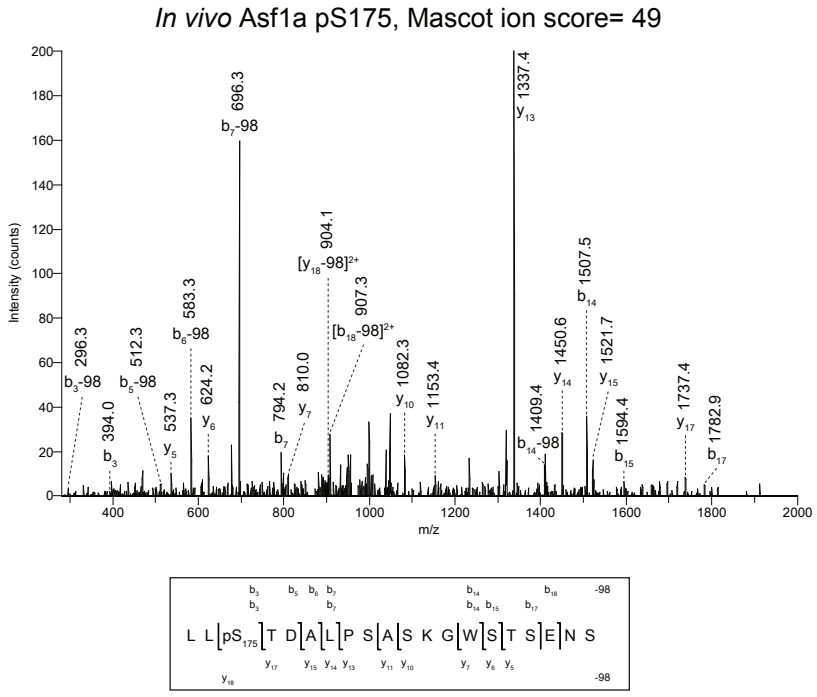

b

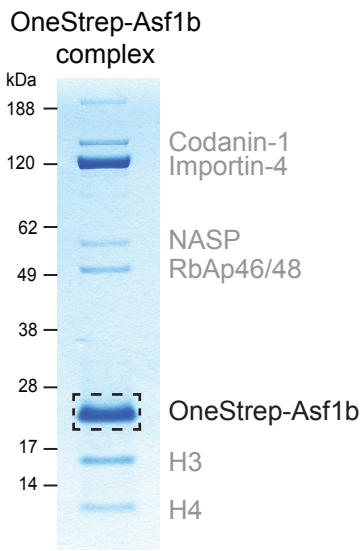

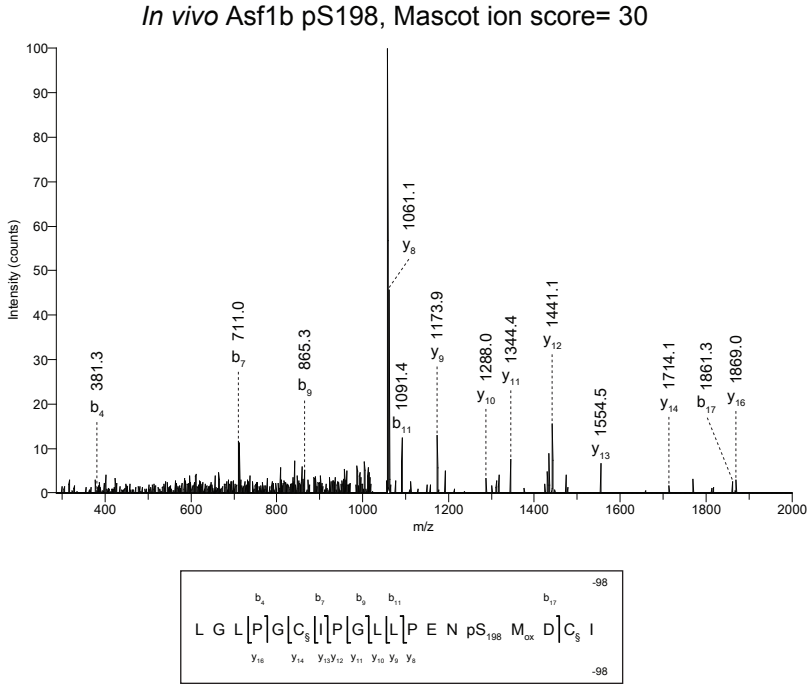

Supplementary Figure 3. Identification of Asf1a and Asf1b *in vivo* phosphorylation sites by mass spectrometry. **(a)** The MS/MS spectra of the Asf1a peptide containing pS175. OneStrep-Asf1a was isolated from asynchronous HeLa S3 cells for LC-MS/MS (see Fig.1b). **(b)** *(Left)* Coomassie staining of cytosolic OneStrep-Asf1b complexes purified from HeLa S3 cells in S phase. The band corresponding to OneStrep-Asf1b (boxed) was analyzed by LC-MS/MS. *(Right)* MS/MS spectra of the Asf1b peptide containing pS198. Observed b- and y-ions, and those resulting from the neutral loss of H_3PO_4 (-98 Da), are indicated. $C_§$ denotes a carbamidomethylated cysteine, M_{ox} represents an oxidized methionine.

Supplementary Figure 4

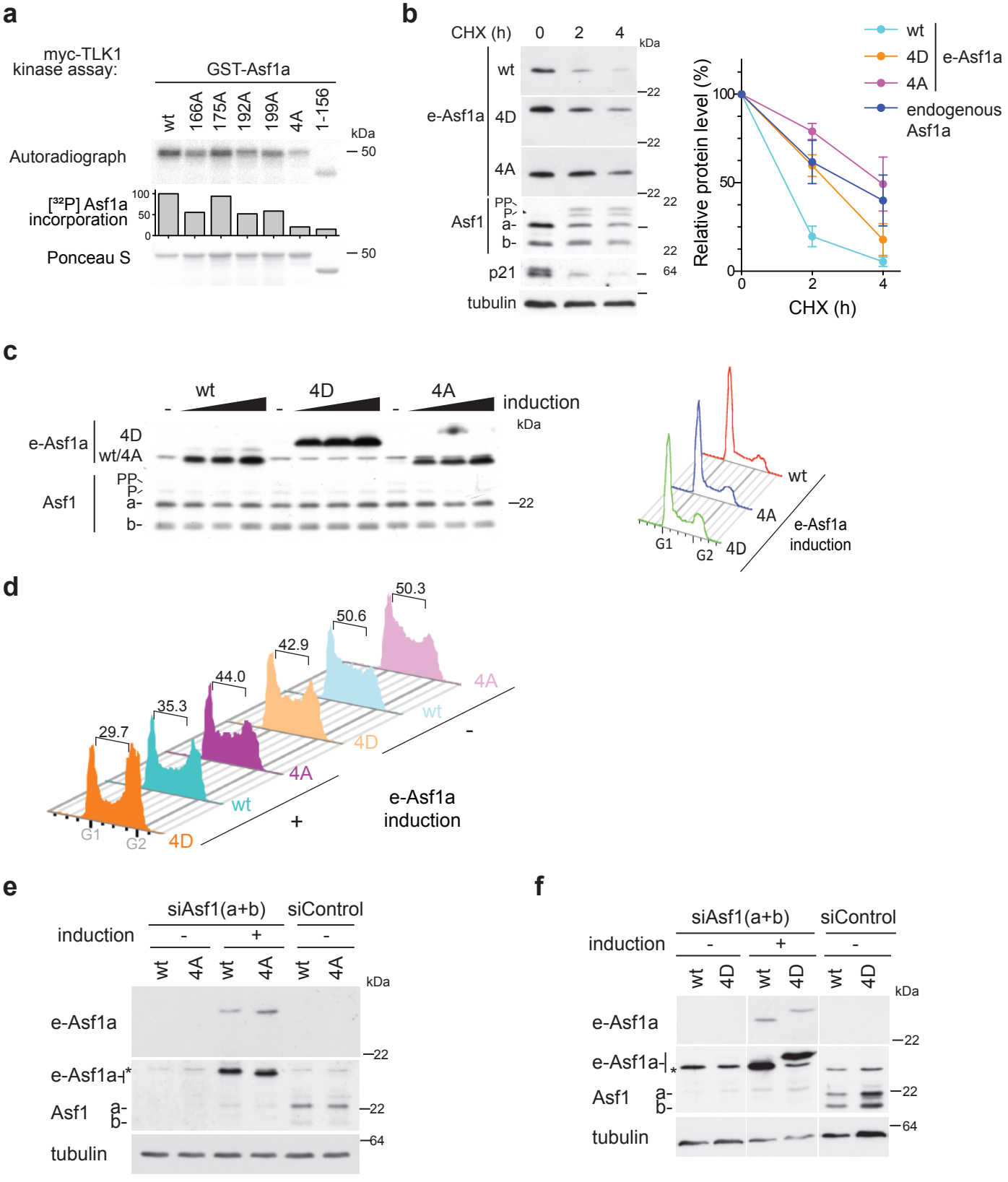

Supplementary Figure 4. Functional analysis of C-terminal Asf1a phosphorylations. (a) In vitro phosphorylation of GST-Asf1a by recombinant myc-TLK1. Asf1a: wt (wild-type, amino acid 1-204), 4A (S166A, S175A, S192A, S199A), **(b)** *(Left)* The stability of Asf1a wild-type (wt), phospho-mimetic (4D) and phosphorylation-deficient (4A) mutants was analyzed in cells treated with cycloheximide (CHX). Flag-HA- Asf1a (e-Asf1a) wt, 4D, 4A were expressed in conditional cell lines for 12 hours and detected by HA antibodies. P and PP denote Asf1a phosphorylation. *(Right)* Quantification of e-Asf1a wt/4D/4A relative protein levels. e-Asf1a levels in untreated cells were set to 100%. Mean protein levels from 3 independent experiments are shown, error bars indicate s.d. Note that the dark blue line indicates total endogenous Asf1a including phospho-forms, which is similar to the 4A and 4D mutant with respect to stability. **(c)** *(Left)* Western blot analysis of exogenous Asf1 (e-Asf1a) overexpression relative to endogenous Asf1 after induction with 1 µg/ml tetracycline for 9, 12 and 16 hours. *(Right)* Cell cycle analysis of cells overexpressing either wild-type Asf1a or phospho-mutants for 16 hours.**(d)** Cell cycle profiles of the experiments described in figure 3a and 3b. Numbers show the proportion of S phase cells. The S phase population was identified by Dean-Jett-Fox model (FlowJo) in the sample treated with control siRNA and the same gates were then imposed on the profiles of Asf1 (a and b) depleted cells. **(e, f)** Western blot showing that e-Asf1a proteins were expressed at the similar levels and endogenous Asf1 (a and b) was efficiently depleted in the experiments described in figures 3d and 3e. Treatment with control siRNA (siControl) and induction of siRNA-resistant forms of e-Asf1a wt/4D/4A after depletion of endogenous Asf1 (a and b) (siAsf1(a+b)) are indicated. *, unspecific band.

Supplementary Figure 5

a

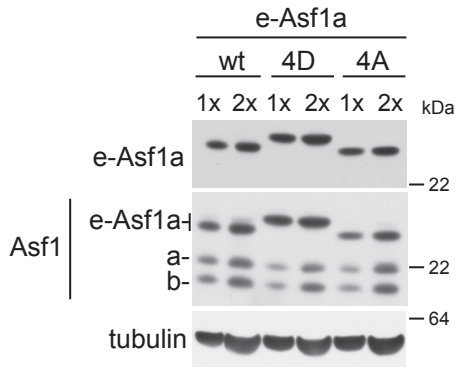

b

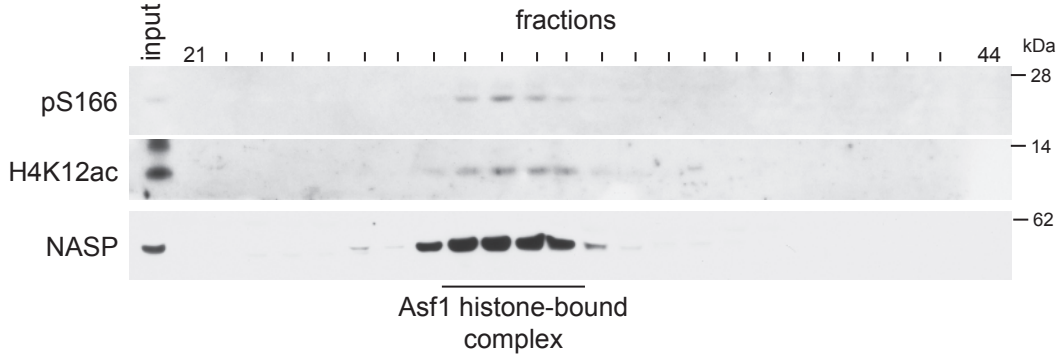

c

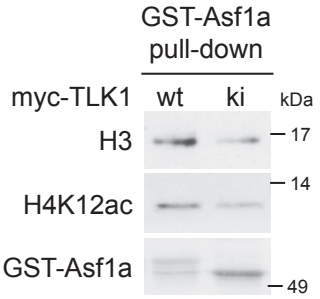

d

pI of Asf1 proteins

	Full-length		Tail		Tailless
	Non-phosphorylated	Phospho/D/E	Non-phosphorylated	Phospho/D/E	
*sc*Asf1	3.88		3.52		4.44
*sp*Asf1	3.73		3.22		4.23
*hs*Asf1a	4.29	4.07/4.17/4.21	4.12	2.92/3.79/3.91	4.37
*hs*Asf1b	4.46	4.33/4.37/4.40	4.02	3.35/3.80/3.89	4.61

Supplementary Figure 5. Phosphorylation enhances Asf1 binding to soluble histones in vivo. **(a)** Western blot showing similar expression of FLAG-HA-Asf1a (e-Asf1a) wild-type (wt), phospho-mimetic (4D) and phosphorylation-deficient mutant (4A) in cytosolic extracts used for the gel-filtration analysis in figure 4b. **(b)** Size-exclusion chromatography of cytosolic extracts prepared from HeLa S3 S phase cells. The histone-bound Asf1 complex is indicated. **(c)** Pull-down with phosphorylated GST-Asf1a in HeLa S3 cells extracts. GST-Asf1a was pre-incubated with recombinant myc-TLK1 wild-type (wt) or kinase-inactive (ki) and used as bait after removal of the kinase. **(d)** Table indicating the isoelectric point (pI) of Asf1 from human *(hsAsf1a/b)*, *S. cerevisiae (scAsf1)* and *S. pombe (spAsf1)*. The calculation of pIs were performed using the online tool Scansite for the full-length proteins, N-terminal domains (tailless), and the C-terminal tails. Additionally, pIs of human Asf1 proteins were calculated considering TLK-mediated phosphorylation or substitution with aspartates or glutamates at TLK-target sites (Asf1a: S166, S175, S192, S199 and Asf1b: S169 and S198).

Supplementary Figure 6

a

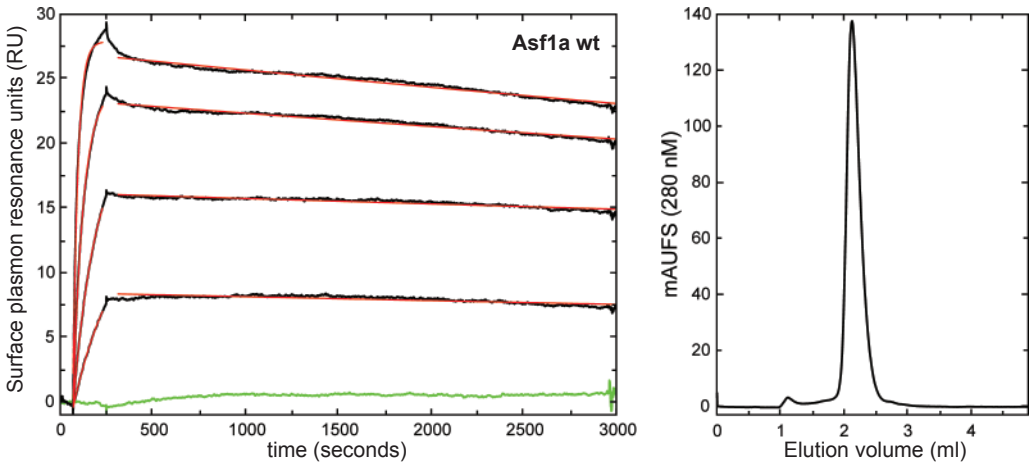

b

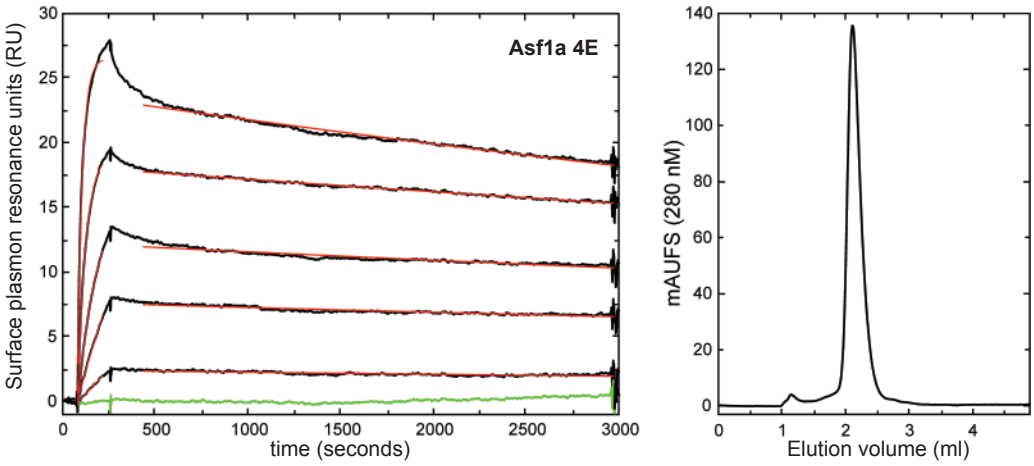

c

***Ligand*[1]**	k_{on} 10^6 $M^{-1}s^{-1}$	k_{off} 10^{-4} s^{-1}	K_d 10^{-12}M	R_{max} RU
Asf1a wt	1.17 ± 0.47	0.45 ± 0.13	46 ± 24	28 ± 6
Asf1a 4E	1.26 ± 0.42	0.89 ± 0.23	79 ± 32	23 ± 7
Asf1a 1-156	2.86 ± 0.77	0.54 ± 0.18	22 ± 15	19 ± 5
Asf1a V94R	nbd[2]	nbd[2]	nbd[2]	0

Supplementary Figure 6. Real-time binding kinetics for the interaction between Asf1a wt or phospho-mimetic mutant (4E) and surface-captured H3.1-H4 by surface plasmon resonance. **(a)** *(Left)* The sensorgrams were recorded for the recombinant Asf1a wt interaction with immobilized recombinant H3.1-H4 in real-time by injecting 3, 8, 24, and 73 nM of Asf1a wt for 200 sec (association phase) and following the dissociation of the formed complexes by changing to buffer flow for the next 2750 sec. The fits from the evaluations are superimposed onto the double referenced data (in red) and the corresponding buffer-run is shown in green. *(Right)* The elution profile from the size exclusion chromatography of Asf1a wt, which is substantiating that purified recombinant Asf1a is a monomer at these conditions. **(b)** Similar to (a) the equivalent data recorded for the Asf1a 4E mutant, including one additional sensorgram recorded for 1 nM Asf1a 4E. Data recorded for Asf1a truncation (1-156) and histone-binding (V94R) mutants are not shown. **(c)** Summary of the kinetic rate constants for the Asf1a-(H3.1-H4) interaction. +/- indicate the SD values obtained for the kinetic rate constants after mathematical fitting using non-linear regression. [1]Three-fold dilution series of the Asf1a ligands were measured at 20°C at a flow rate of 20 µl/min, and covering the concentration range from 1 to 73 nM. Long dissociation phases (45 minutes) were included due to the tight binding of these ligands. [2]nbd: no specific binding was detected for Asf1a V94R mutant.

Supplementary Figure 7

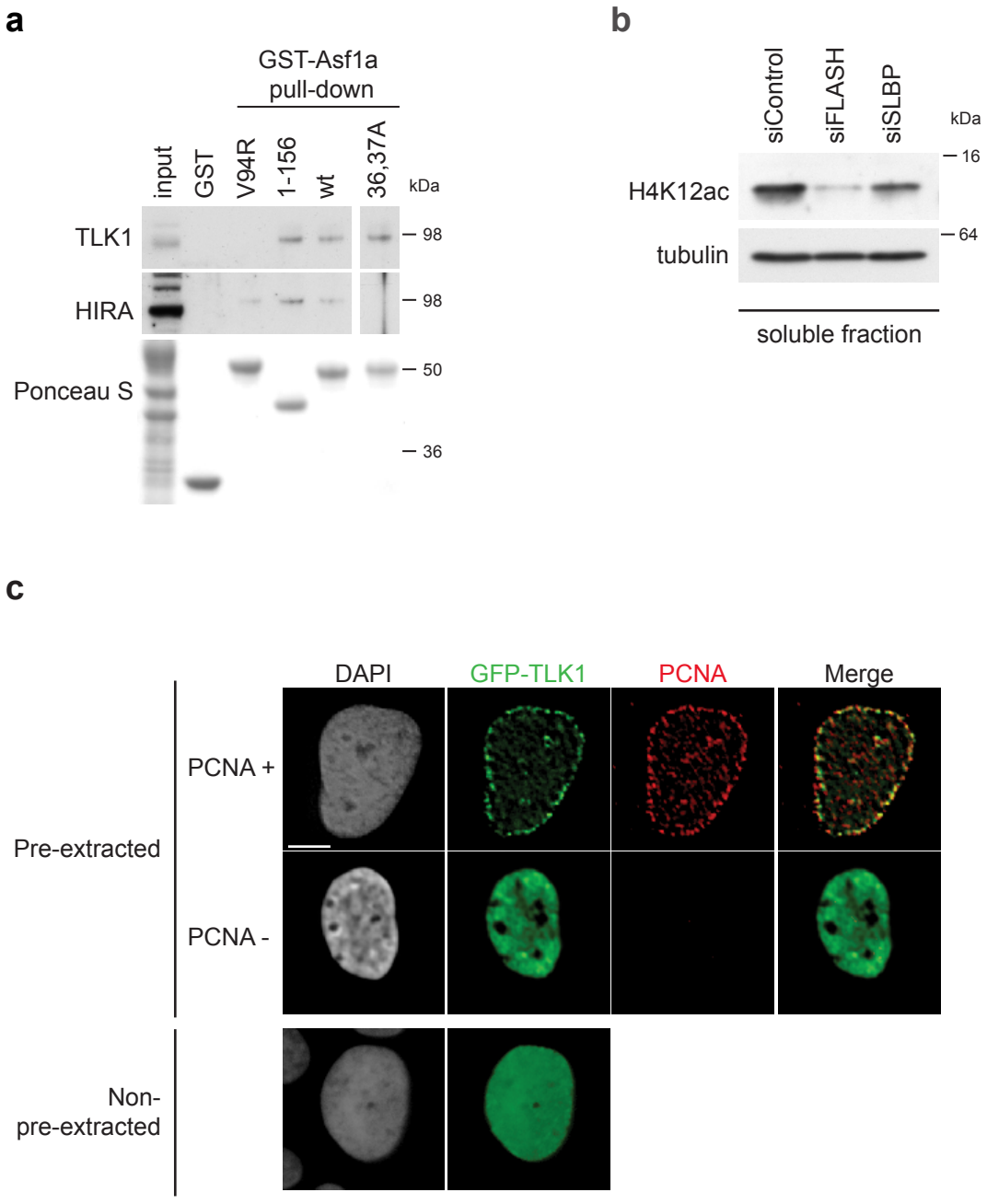

Supplementary Figure 7. TLK binding to Asf1 requires an intact histone-binding pocket. **(a)** GST-Asf1a pull-downs comparing full-length (wt) and truncated (1-156) Asf1a with histone-binding (V94R)1 and B-domain (36,37A)2 mutants. Binding of TLK1 and HIRA in total U-2-OS cell extracts was analyzed by western blot. **(b)** Depletion of FLASH (siFLASH) or SLBP (siSLBP) reduces the pool of soluble histones. The level of soluble histone H4 carrying K12ac was assessed by western blotting. **(c)** Immunofluorescence analysis of GFP-TLK1 in conditional U-2-OS cells. GFP-TLK1 distribution was analyzed after pre-extraction of soluble proteins and in cells directly fixed with paraformaldehyde. Co-staining with PCNA in pre-extracted cells was used to mark replication sites. In pre-extracted cells, GFP-TLK1 shows either foci co-localizing with PCNA or pan nuclear distribution in PCNA negative cells. Nuclei were stained with DAPI. Scale bar is 5 μm.

Supplementary Figure 8

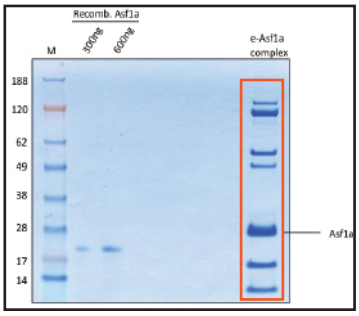

Fig.1b

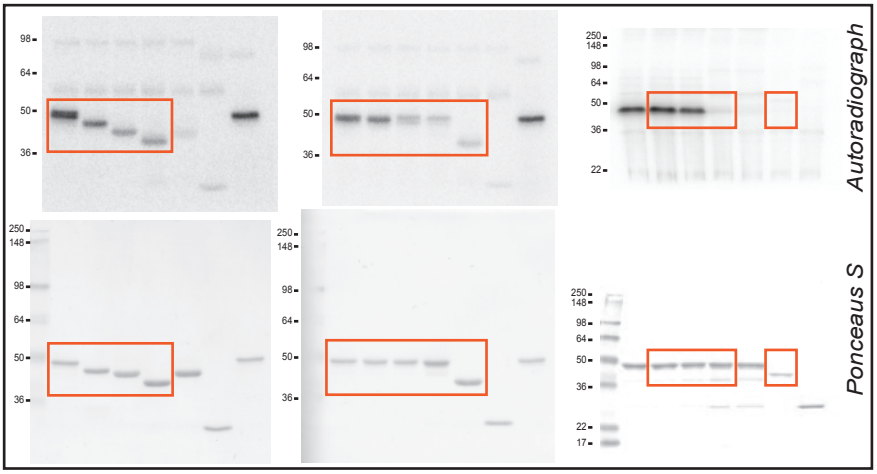

Fig. 1c

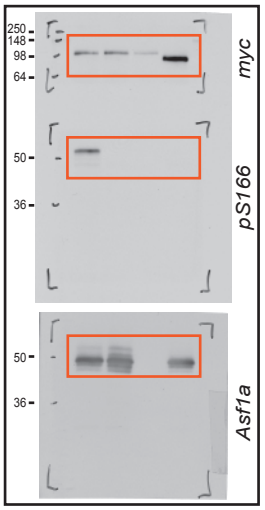

Fig. 1d

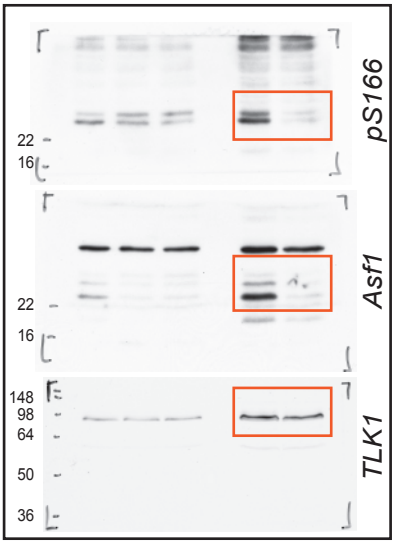

Fig.1e

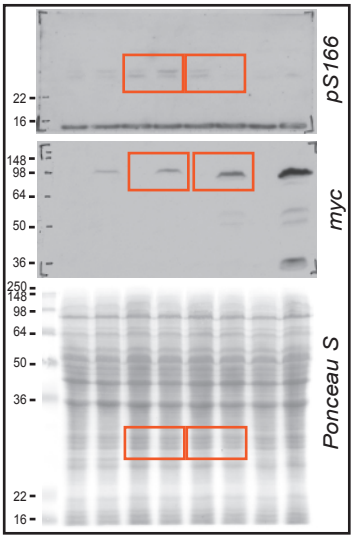

Fig. 1f

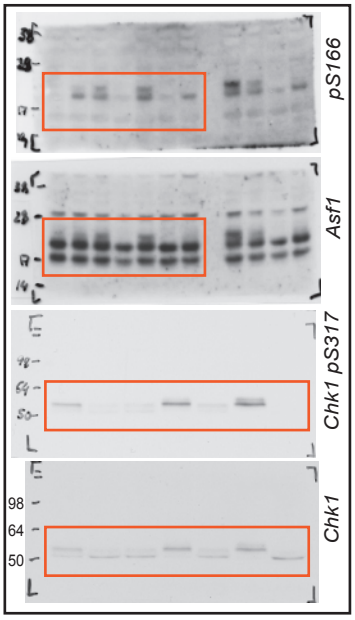

Fig. 2a (left)

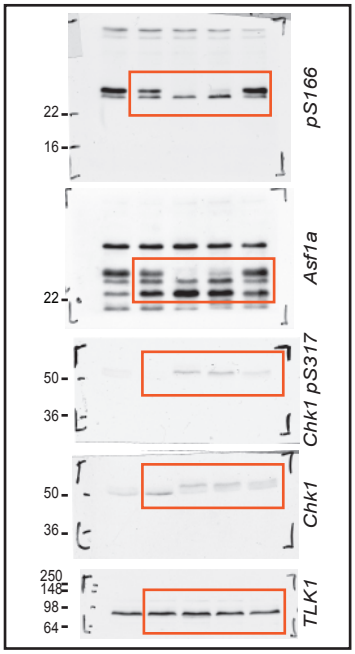

Fig. 2c

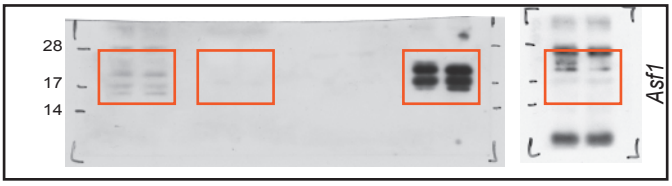

Fig. 2a (right)

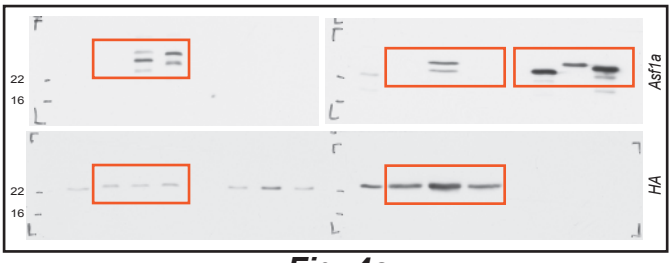

Fig. 4c

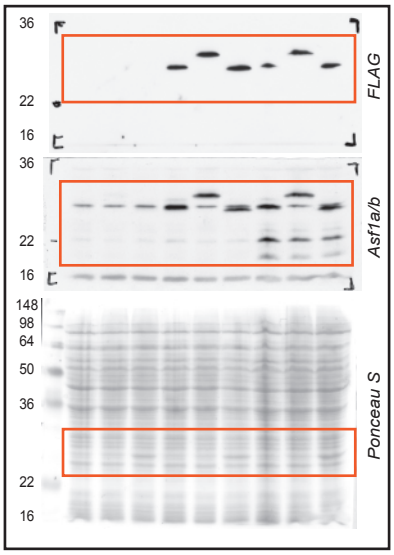

Fig. 3a

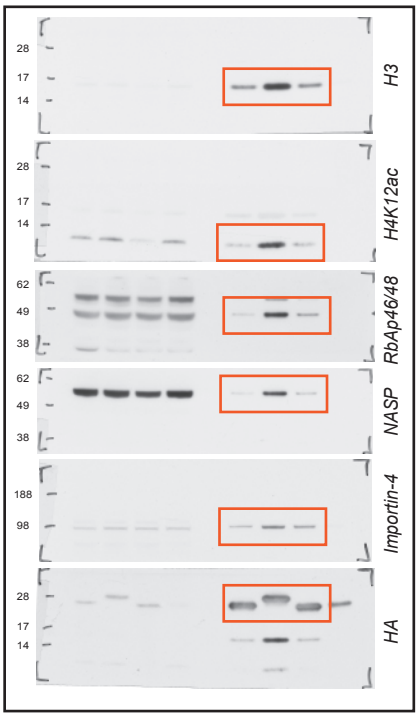

Fig. 4a

Supplementary Figure 8. Full scan of gels and blots used in the manuscript. Boxed regions correspond to portion used in the figures.

Supplementary Figure 9

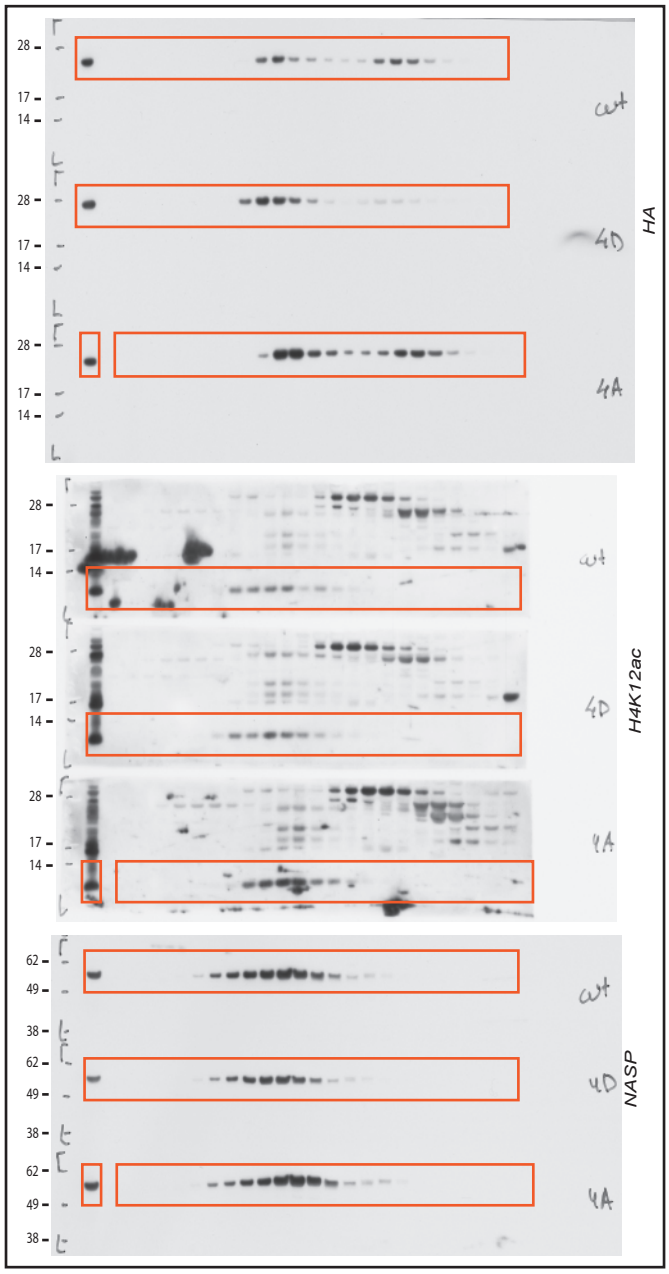

Fig. 4b

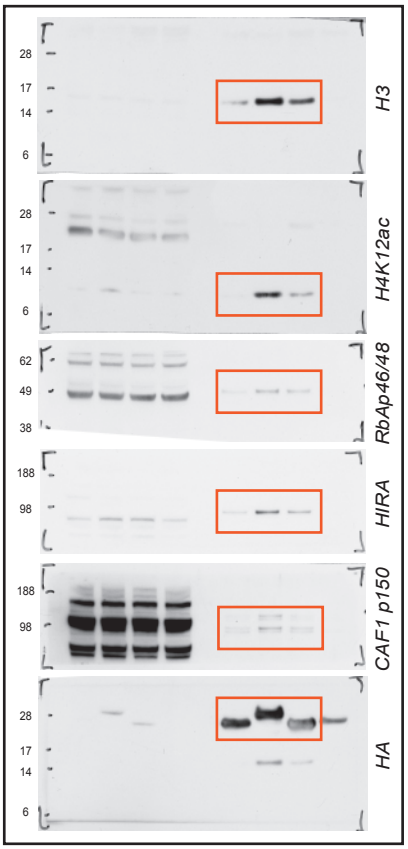

Fig. 5a

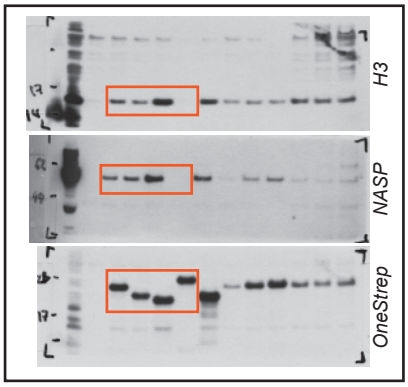

Fig. 5e

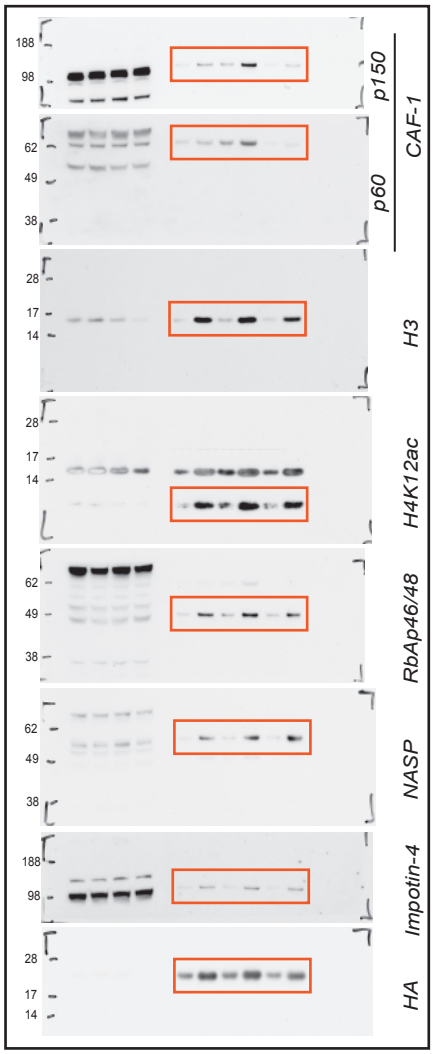

Fig. 5c

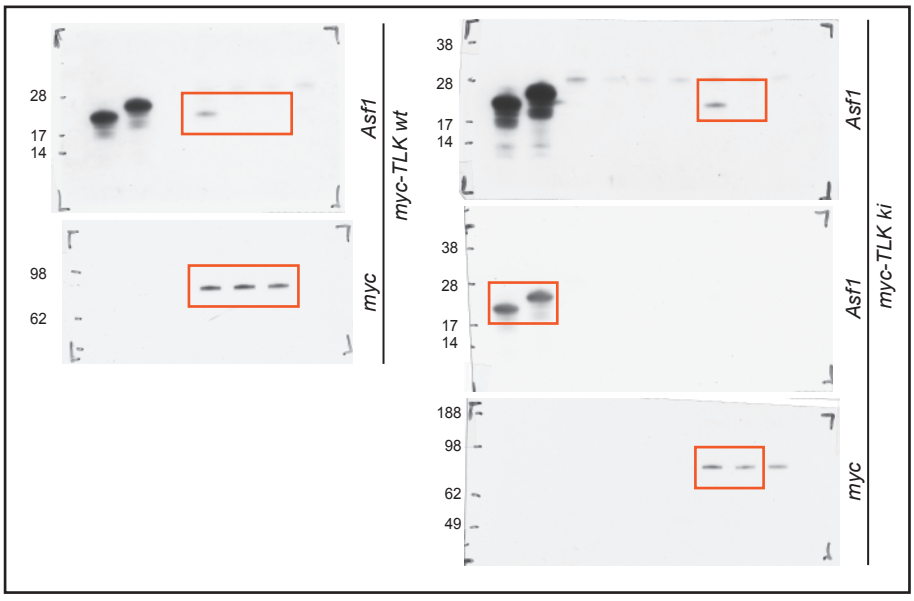

Fig. 6a

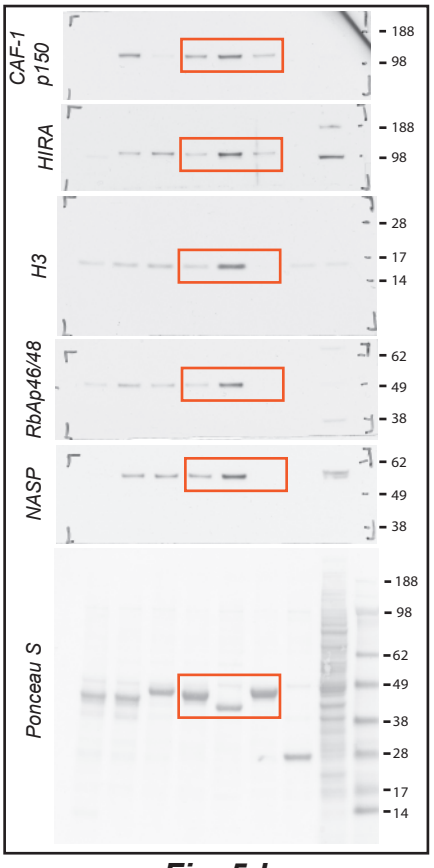

Fig. 5d

Supplementary Figure 9. Full scan of gels and blots used in the manuscript. Boxed regions correspond to portion used in the figures.

Supplementary Figure 10

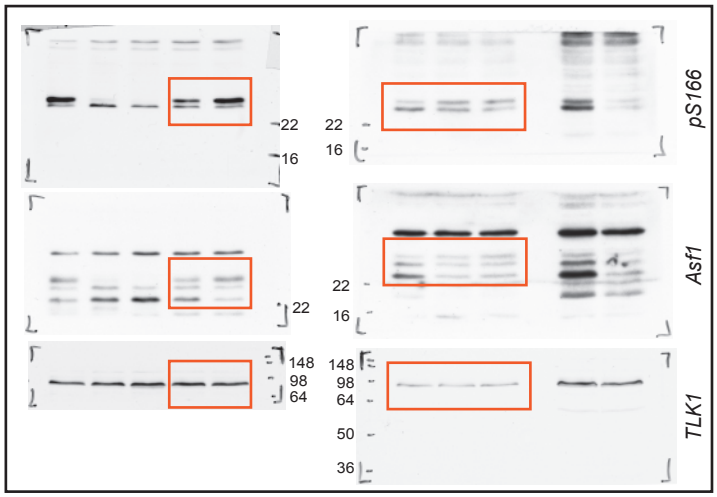

Fig. 6b

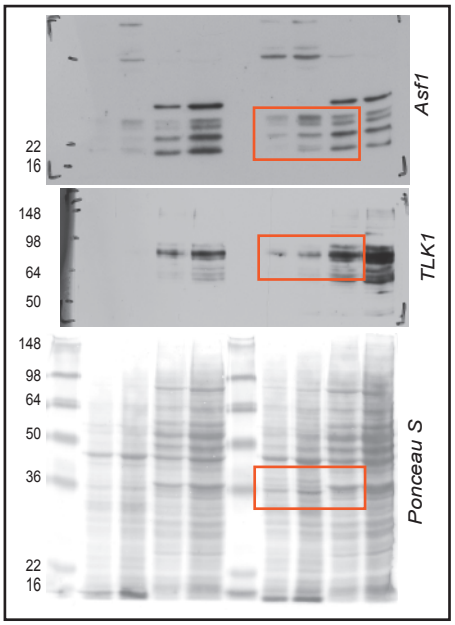

Fig. 6c

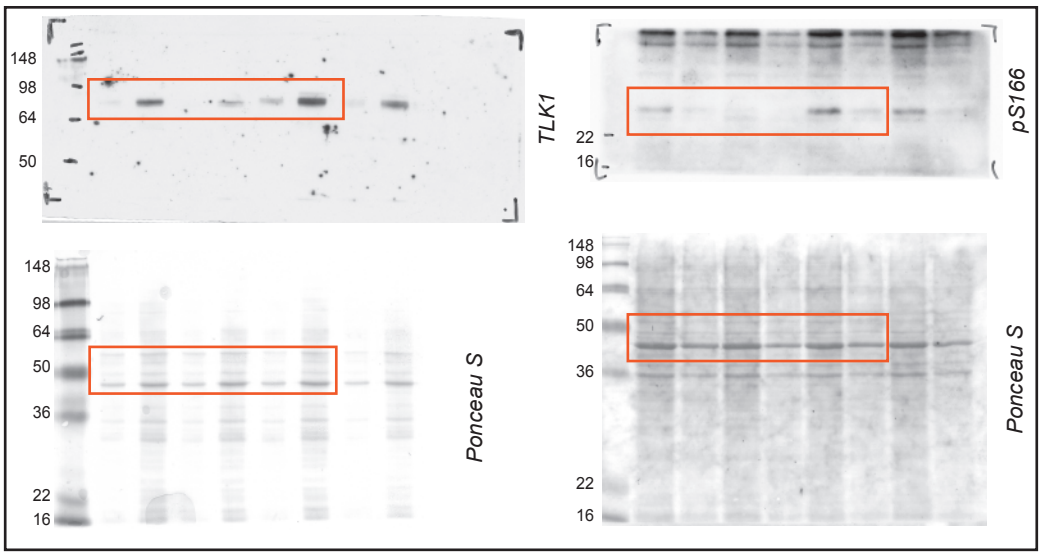

Fig. 6d

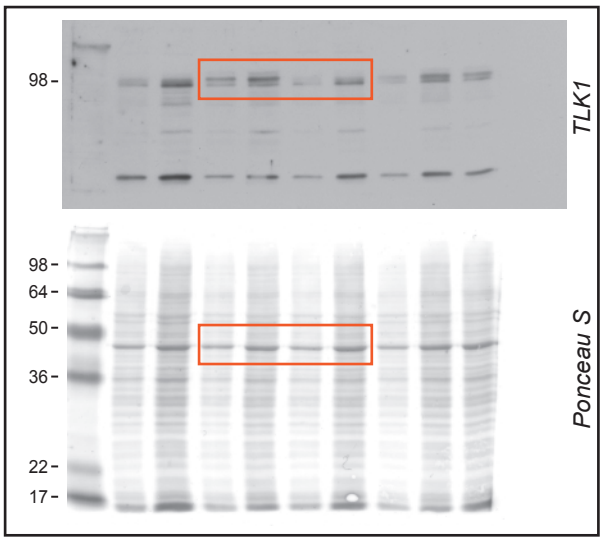

Fig. 6e

Supplementary Figure 10. Full scan of gels and blots used in the manuscript. Boxed regions correspond to portion used in the figures.

SUPPLEMENTARY TABLES

Supplementary Table 1. Plasmids used in this study.

Plasmid constructs	References
pcDNA5/FRT/TO-FLAG-HA-Asf1a	*This study*
pcDNA5/FRT/TO-FLAG-HA-Asf1a (4D)	*This study*
pcDNA5/FRT/TO-FLAG-HA-Asf1a (4A)	*This study*
pcDNA5/FRT/TO-FLAG-HA-Asf1b	*This study*
pcDNA5/FRT/TO-FLAG-HA-Asf1b (2E)	*This study*
pcDNA5/FRT/TO-FLAG-HA-Asf1b (2A)	*This study*
pGEX-6P-3-Asf1a	[1]
pGEX-6P-3 Asf1a (1-156)	[2]
pGEX-6P-3 Asf1a (1-174)	*This study*
pGEX-6P-3 Asf1a (1-186)	*This study*
pGEX-6P-3-Asf1a S166A	*This study*
pGEX-6P-3-Asf1a S175A	*This study*
pGEX-6P-3-Asf1a S192A	*This study*
pGEX-6P-3-Asf1a S199A	*This study*
pGEX-6P-3-Asf1a (2A)	*This study*
pGEX-6P-3-Asf1a (3A)	*This study*
pGEX-6P-3-Asf1a (4A)	*This study*
pGEX-6P-3-Asf1a (4E)	*This study*
pGEX-6P-3-Asf1a (V94R)	*This study*
pGEX-6P-3 Asf1a (36,37A)	*This study*
pGEX-6P-3-Asf1b	[1]
pGEX-6P-3-Asf1b S198A	*This study*
pGEX-6P-3-Asf1b S169A	*This study*
pGEX-6P-3-Asf1b (2A)	*This study*
pGEX-6P-3-Asf1b (1-157)	*This study*
pGEX-6P-3 Asf1b (36,37A)	[3]
pEXPR-IBA105-Asf1a	[4]
pEXPR-IBA105-Asf1a (1-186)	*This study*
pEXPR-IBA105-Asf1a (1-174)	*This study*
pEXPR-IBA105-Asf1a (V94R)	[4]
pVL1392 myc-TLK1	[5]
pVL1392 myc-TLK1 D559A	[5]
pBluescript myc-TLK1	[5]
pBluescript myc-TLK1 D559A	[5]
pBI myc-GFP-TLK1	[6]
pRcCMV	Invitrogen

Supplementary Table 2. Cell lines used in this study

Cell lines	Reference	Maintenance
U-2-OS Flp-In T-REx (U-2-OS Flp-In)	Kindly provided by J. Nilsson	Zeo + Blast
U-2-OS Flp-In e-Asf1a	*This study*	Hyg + Blast
U-2-OS Flp-In e-Asf1a (4D)	*This study*	Hyg + Blast
U-2-OS Flp-In e-Asf1a (4A)	*This study*	Hyg + Blast
HeLa S3	Kindly provided by P. Nakatani	
HeLa S3 OneStrep-Asf1a	[4]	G418
HeLa S3 OneStrep-Asf1b	[4]	G418
U-2-OS myc-GFP-TLK1	[6]	Puro+G418+tet
U-2-OS myc-TLK1	[6]	Puro+G418+tet
U-2-OS myc-TLK1ki	[6]	Puro+G418+tet
HeLa S3 H3.1-FLAG-HA	[7]	

Supplementary Table 3. Primary antibodies used in this study

Antibody	Company/reference	Clone/ catalogue number	Dilution
Asf1a pS166	*This study*		1:30000
Asf1	[8]		1:2000
CAF-1 p60	[9]		1:1000
CAF-1 p150	[9]		1:3000
Chk1	Kind gift of Dr. C. Sørensen	Clone DCS310	1:2000
pChk1	Cell Signaling	2344	1:500
HIRA	Abnova	PAB4861	1:50
Histone H3	Abcam	ab1791	1:1000
Histone H4K12ac	Upstate-Millipore	07-595	1:3000
Importin-4	Abcam	ab28387	1:500
sNASP	Kind gift of Dr. O'Rand		1:2000
p21	Santa Cruz	sc-6246	1:1000
PCNA	Abcam	ab29	1:1000
RbAp46/48	Abcam	ab1766	1:2000
TLK1	*This study*		1:3000
α-Tubulin	Sigma	T9026	1:2000
FLAG M2	Sigma	F3156	1:1000
HA	Roche	1867423	1:1000
myc	Kind gift of Dr. J. Bartek	Clone 9E10	1:1000

SUPPLEMENTARY REFERENCES

1. Sillje, H.H. & Nigg, E.A. Identification of human Asf1 chromatin assembly factors as substrates of Tousled-like kinases. *Curr Biol* **11**, 1068-73 (2001).
2. Mousson, F. et al. Structural basis for the interaction of Asf1 with histone H3 and its functional implications. *Proc Natl Acad Sci U S A* **102**, 5975-80 (2005).
3. Ask, K. et al. Codanin-1, mutated in the anaemic disease CDAI, regulates Asf1 function in S-phase histone supply. *EMBO J* **31**, 2013-23 (2012).
4. Groth, A. et al. Regulation of replication fork progression through histone supply and demand. *Science* **318**, 1928-31 (2007).
5. Sillje, H.H., Takahashi, K., Tanaka, K., Van Houwe, G. & Nigg, E.A. Mammalian homologues of the plant Tousled gene code for cell-cycle-regulated kinases with maximal activities linked to ongoing DNA replication. *EMBO J* **18**, 5691-702 (1999).
6. Groth, A. et al. Human Tousled like kinases are targeted by an ATM- and Chk1-dependent DNA damage checkpoint. *EMBO J* **22**, 1676-87 (2003).
7. Tagami, H., Ray-Gallet, D., Almouzni, G. & Nakatani, Y. Histone H3.1 and H3.3 complexes mediate nucleosome assembly pathways dependent or independent of DNA synthesis. *Cell* **116**, 51-61 (2004).
8. Groth, A. et al. Human Asf1 Regulates the Flow of S Phase Histones during Replicational Stress. *Mol Cell* **17**, 301-11 (2005).
9. Green, C.M. & Almouzni, G. Local action of the chromatin assembly factor CAF-1 at sites of nucleotide excision repair in vivo. *EMBO J* **22**, 5163-74 (2003).